

# Prediction of Material Properties of Nanostructured Polymer Composites Using Atomistic Simulations

T. C. Clancy<sup>1</sup> and S. J. V. Frankland<sup>2</sup>

*National Institute of Aerospace, Hampton, VA, 23666, USA*

J. A. Hinkley<sup>3</sup>

*NASA Langley Research Center, Hampton, VA, 23681, USA*

Atomistic models of epoxy polymers were built in order to assess the effect of structure at the nanometer scale on the resulting bulk properties such as elastic modulus and thermal conductivity. Atomistic models of both bulk polymer and carbon nanotube polymer composites were built. For the bulk models, the effect of moisture content and temperature on the resulting elastic constants was calculated. A relatively consistent decrease in modulus was seen with increasing temperature. The dependence of modulus on moisture content was less consistent. This behavior was seen for two different epoxy systems, one containing a difunctional epoxy molecule and the other a tetrafunctional epoxy molecule. Both epoxy structures were crosslinked with diamine curing agents. Multifunctional properties were calculated with the nanocomposite models. Molecular dynamics simulation was used to estimate the interfacial thermal (Kapitza) resistance between the carbon nanotube and the surrounding epoxy matrix. These estimated values were used in a multiscale model in order to predict the thermal conductivity of a nanocomposite as a function of the nanometer scaled molecular structure.

## I. Introduction

There has been a great deal of research effort in recent years on the subject of nanostructured materials.<sup>1</sup> Structure across a range of length scales has been of particular interest. Among materials under study are nanocomposites, in which a particle with at least one dimension on the order of a nanometer is embedded in a polymer matrix. Polymers themselves are 'nanostructured' since they exhibit relevant structural features down at the nanometer length scale. Polymers are high molecular weight macromolecules, which leads to a variety of structural features in the condensed phase. In addition, the presence of contaminants such as moisture will contribute to the molecular structure of the polymeric system. In this paper, results are presented on atomistic simulations of epoxy polymers which are highly crosslinked macromolecular structures. These simulations are used to calculate macroscopic properties such as mechanical elastic constants and thermal conductivity. This is done with the goal of gaining insight into the way in which nanometer scaled structure influences macroscopic properties. Atomistic simulations of polymers in which the elastic constants are calculated have been performed for some time.<sup>2,3</sup> However, atomistic simulations of crosslinked polymers have only been developed in recent years.<sup>4</sup> There have not been many fully atomistic simulations of crosslinked polymers in which mechanical properties have been calculated as a function of molecular structure. Multiscale simulations of thermal properties of polymer nanocomposites have been studied previously.<sup>5-7</sup> In the thermal part of this work, the focus is on the effect of functionalization of the carbon nanotube within an epoxy matrix.

---

<sup>1</sup> Senior Research Scientist.

<sup>2</sup> Senior Research Scientist and AIAA Member.

<sup>3</sup> Physical Chemist, Advance Materials and Processing Branch.

## II. Method

### A. Building atomistic structures

Epoxies are crosslinked polymer materials which are formed from the reaction of molecules which have epoxide groups and crosslinker molecules. In this paper, two types of epoxide containing molecules are used in simulations, a difunctional epoxy and a tetrafunctional epoxy. Figure 1 shows the two different epoxy types. In Figure 1a, the molecular structure of the diglycidyl ether of bisphenol A (DGEBA) is depicted. In Figure 1b, the structure of tetraglycidyl diamino diphenyl methane (TGDDM) is depicted. The tetrafunctional epoxy contains four epoxy groups, leading to a potentially higher number of crosslinks per unit volume than the difunctional epoxy. In Figure 2, the molecular structures of the crosslinkers used in the simulation are depicted. In Figures 2a-b, the structures of the two isomers of diethylene toluene diamine (DETDA) are depicted. In Figure 2c, the structure of diamino diphenyl sulfone (DDS) is depicted. Each of these crosslinkers contains two amine groups which can react with the epoxide. In some simulations, water ( $H_2O$ ) is also included in the simulation as a contaminant. In addition, a carbon nanotube (CNT) is also simulated with an epoxy in some of the simulations. The nanotube is functionalized by the chemical bonding of a functional group to the surface of the CNT. This functional group is an amide which contains an amine group that can participate in the crosslinking reaction. Figure 3a shows the chemical reaction of a crosslinking molecule containing an amine group reacting with a molecule containing an epoxide functional group. Figure 3b illustrates the product of the reaction from Figure 3a reacting with a second epoxide group. These reactions lead to the formation of highly crosslinked macromolecular structures. A mixture of an epoxy and a crosslinker will react according to the reactions depicted in Figure 3 to produce the cured epoxy network. In simulations in which a CNT is present, the CNT is simulated as extending through the periodic boundary conditions (PBC) in one of the directions. Further details on the construction of these atomistic epoxy models and of these nanocomposites have been presented previously.<sup>5,8</sup> In this paper, results are presented from calculations performed on three structural types. The first two contained only cured epoxy with varying amounts of water added. The first of these was a DGEBA-DETDA epoxy. The second of these was a TGDDM-DDS epoxy. The third type built was a DGEBA-DDS epoxy with a CNT. No water was added to the CNT-epoxy nanocomposite.

### B. Molecular Dynamics simulation details

In simulating these atomistic structures, the LAMMPS<sup>9</sup> software was used to run these molecular mechanics (MM) and molecular dynamics (MD) simulations. The force field used was AMBER<sup>10,11</sup> while the TIP3P<sup>12</sup> parameters were used to simulate water. A bond decrement method used for the CVFF force field in the Materials Studio software was used to estimate partial charges.<sup>13</sup> The unreacted epoxy and crosslinker molecules (including the CNT if present) were simulated in the condensed phase prior to crosslinking. The epoxy and crosslinker are present in a stoichiometrically equivalent ratio. This condensed phase reactant mixture was simulated with MD for  $2 \times 10^5$  time steps (200 ps) using a 1 fs time step. This duration of MD time step was used in all the MD simulations. A final equilibrated configuration was taken and used for the construction of the crosslinked epoxy.

Using this final static configuration of atomic coordinates of the condensed phase reactant mixture, a crosslinked network is formed by the addition of chemical bonds consistent with the chemical reactions depicted in Figure 3. The epoxide groups react with the amine groups to form chemical bonds. This results in a complex network structure. The method used is essentially that employed by most researchers for constructing atomistic crosslinked structures.<sup>4,14</sup> This new crosslinked structure is then used for the MM/MD simulation.

The newly created atomistic configuration must be carefully equilibrated since the initial configuration is initially far from equilibrium. A short initial energy minimization is applied to the structure using a conjugate gradient algorithm in the LAMMPS software with an energy delta tolerance of  $10^{-4}$  kcal/mol. This is followed by an isothermal-isobaric MD simulation at a temperature of 300 K and a pressure of 1 atm for  $2 \times 10^5$  time steps (200 ps). The network formation procedure can be repeated in order to increase the degree of crosslinking. The degree of crosslink,  $\alpha$ , is a fraction of the number of epoxide groups which have reacted to become part of the network. In this stoichiometrically equivalent mixture, the maximum value for  $\alpha$  is 1, which corresponds to all of the epoxides reacting with an amine. Once the desired degree of crosslinking,  $\alpha$ , is achieved, a more complete equilibration is applied. An energy minimization procedure is applied with a restriction of energy delta tolerance of  $10^{-4}$  kcal/mol. The structure was simulated with MD for  $10^5$  time steps ( $10^2$  ps) starting at a high temperature under isothermal-isobaric conditions. The structures were then cooled in a stepwise manner to achieve equilibrated structures over a range of temperatures. In the simulation of epoxy with no CNT present, the structures had water introduced in small percentages. The water molecules were added randomly to the structures. Following the addition of water molecules, energy minimization was applied. The structures were then subsequently equilibrated with MD using a stepwise cooling procedure described in the previous paragraph.

In order to obtain additional configurations for running deformation simulations, the MD simulation was run for an additional 100 ps. The final trajectory at each temperature is saved for running deformation simulations. The MD simulation was repeated for another 100 ps in order to obtain 3 separate atomistic configurations with their associated velocities for a given degree of crosslinking ( $\alpha$ ), moisture content ( $f_{water}$ ), and temperature ( $T$ ). Although an MD run of this length ( $10^5$  time steps,  $10^2$  ps) does not result in drastically distinct configurations, the properties calculated from these configurations did show statistical variation.

### C. Calculation of mechanical properties

The elastic constants are calculated by monitoring the stress tensor while deforming the periodic boundary conditions during a MD simulation. This is similar to an established method which used static models,<sup>2</sup> but here is applied in a constant volume-constant temperature (NVT) ensemble. The 6x6 elastic constant matrix  $\mathbf{C}$  is determined by the partial derivatives of the stress tensor,  $\tau$ , with respect to the deformation,  $\epsilon$ , as indicated by Equation 1.

$$C_{LMNK} = \left. \frac{\partial \tau_{LM}}{\partial \epsilon_{NK}} \right|_{T, \epsilon(NK)} \quad (1)$$

Three uniaxial tension deformations and three shear deformations are applied to each model. An isotropic symmetry is assumed, and the constants are averaged over the various orientations. The deformations were applied in a continuous fashion at every time step at a constant rate with respect to the original dimensions. The periodic boundary cell was deformed in a positive direction by 5% over a simulation period of  $10^2$  ps ( $10^5$  time steps). These are typical rates of deformations for MD simulations and are necessary due to the limitation of the MD simulation method.<sup>15,16</sup> The stress tensor was recorded at 10 time step (10 fs) intervals leading to a collection of  $10^4$  data points which were then averaged in batches of  $10^3$  time step intervals (10 ps). A least squares fitting method is used to obtain the elastic constants,  $\mu$  and  $\lambda$  from Equations 2-6.<sup>3</sup> Here, the contracted notation for the  $\mathbf{C}$  matrix is used.

$$\mu = \frac{4a - 2b + 3c}{33} \quad (2)$$

$$\lambda = \frac{2a + c - 15\mu}{6} \quad (3)$$

$$a = C_{11} + C_{22} + C_{33} \quad (4)$$

$$b = C_{12} + C_{13} + C_{21} + C_{23} + C_{31} + C_{32} \quad (5)$$

$$c = C_{44} + C_{55} + C_{66} \quad (6)$$

The Young's modulus,  $E$ , and shear modulus,  $G$ , can then be calculated from Equations 7-8.

$$E = \mu \frac{3\lambda + 2\mu}{\lambda + \mu} \quad (7)$$

$$G = \mu \quad (8)$$

### D. Estimating the interfacial thermal resistance and thermal conductivity

A multiscale modeling approach is used to estimate the thermal conductivity of CNT nanocomposites. Atomistic simulation is used to predict the interfacial thermal resistance between the CNT and the surrounding epoxy matrix. The interfacial thermal resistance was calculated<sup>6,7,17</sup> by instantaneously heating the nanoparticle atoms to a temperature of 500 K and then monitoring the difference in temperature,  $\Delta T$ , between the nanoparticle atoms and the matrix atoms during a constant energy simulation (NVE ensemble). These data are then plotted as the natural logarithm of  $\Delta T$  vs. time yielding a slope which is the negative inverse of the characteristic decay time,  $\tau$ . Equation 9 then gives the interfacial thermal resistance,  $R_K$ , where  $c_T/A_T$  is the heat capacity per area of nanoparticle

surface. This ratio ( $c_T/A_T$ ) is calculated assuming a value of 0.71 J/gK for  $c_T$ .<sup>18</sup> This results in a value of  $5.6 \times 10^{-4}$  J/m<sup>2</sup>K for  $c_T/A_T$  for the CNT.

$$R_K = \frac{\tau}{(c_T/A_T)} \quad (9)$$

These interfacial resistance values from the heat transfer simulations are then used in an analytical formula<sup>19</sup> to calculate the thermal conductivities of nanocomposites. While molecular modeling yields  $R_K$  values, an analytical model is applied in order to calculate the thermal conductivity of the nanocomposite material. This approach is taken because of the range of length scales that are relevant in the properties that are calculated. The interfacial thermal resistance depends on nanometer length scaled features of the nanocomposite and as such it is more reasonable to use a nanometer scaled modeling approach (MD). Thermal conductivity is a macroscopic property and a model is required which links nanometer scaled information (interfacial thermal resistance) with large length scaled features. This model assumes a random orientation of the dispersed nanotubes within the polymer matrix and uses an effective medium approach. This approach yields a formula for calculating the thermal conductivities of CNT composites.<sup>19</sup> This is summarized by Equations 10-13.

$$K_e = K_m \frac{3 + f(\beta_x + \beta_z)}{2 - f\beta_x} \quad (10)$$

$$\beta_x = \frac{2(K_{11}^c - K_m)}{K_{11}^c + K_m}, \quad \beta_z = K_{33}^c / K_m - 1 \quad (11)$$

$$K_{11}^c = \frac{K_c}{1 + \frac{2a_k}{d} \frac{K_c}{K_m}}, \quad K_{33}^c = \frac{K_c}{1 + \frac{2a_k}{L} \frac{K_c}{K_m}} \quad (12)$$

$$a_k = R_K K_m \quad (13)$$

Material properties  $K_e$ ,  $K_c$ , and  $K_m$  are the thermal conductivities of the nanocomposite, the CNT and the polymer matrix, respectively. In evaluating Equations 10-13, a value of 0.2 W/mK is used for  $K_m$ . A value of 6000 W/mK is used for  $K_c$ .<sup>20</sup> The diameter of the (8,8) SWCNT,  $d$ , is 1.077 nm,  $L$  is the nanotube length (assumed to be  $10^{-4}$  m), while  $f$  is the volume fraction, and  $a_k$  is the Kapitza radius.

### III. Results

#### A. Mechanical properties of the epoxy simulations

Figure 4 shows the Young's modulus for the TGDDM-DDS epoxy as a function of temperature for three different water contents. Figure 5 shows the Young's modulus for the DGEBA-DETDA epoxy as a function of temperature for three different water contents. In both cases, the modulus decreases consistently with increasing temperature. The modulus of the TGDDM-DDS epoxy is much higher than that of the DGEBA-DETDA at comparable values  $\alpha$ ,  $f_{water}$  and  $T$ . However, since  $\alpha$  is defined in terms of the degree to which the crosslinking chemical reaction proceeds and the TGDDM molecule contains twice as many epoxide groups as the DGEBA molecule, this parameter ( $\alpha$ ) is a bit misleading. The TGDDM-DDS model ( $\alpha = 0.875$ ) has density of about 1.8 crosslinks/nm<sup>3</sup>, whereas the DGEBA-DETDA ( $\alpha = 0.86$ ) model has a density of about 1.3 crosslinks/nm<sup>3</sup>. The increased number of actual crosslinks per unit volume is likely an important factor in the higher modulus of the tetrafunctional cured epoxy (TDDDM-DDS) versus the difunctional cured epoxy (DGEBA-DETDA). Figure 6 shows the Young's modulus as a function of water fraction  $f_{water}$  (in wt. %) for the TGDDM-DDS epoxy model while Figure 7 shows the Young's modulus as a function of  $f_{water}$  for the DGEBA-DETDA system. Here, the behavior does not seem quite as consistent as far as the Young's modulus having a simple dependence on the water content. Although in general the moduli tend to decrease with increasing water content at the higher temperatures, there seems to be cases where the modulus actually appears to increase with increased water content. We have to consider several possibilities. One is that under certain conditions water may act as a plasticizer resulting in a decrease in modulus, and yet under other conditions, it may act as an anti-plasticizer causing an increase in modulus. Both conditions have been cited from experimental measurements in the literature.<sup>21</sup> The possibility exists that

under the high strain rates inherent in the MD simulation process, the relaxation mechanisms are different, resulting in discrepancies. There have been detailed analyses of the water-polymer matrix structure offered which suggest roles that various features such as free volume and the role of water molecules within the matrix have on these properties.<sup>22</sup> However, the possibility exists as well that these results are simply a matter of insufficient statistical sampling in these models.<sup>22</sup> In any case, we do not attempt to analyze this situation further within the current text.

The effect that the degree of crosslinking has on volumetric properties was examined for the TGDDM-DDS epoxy. Figure 8 shows the specific volume for a TGDDM-DDS epoxy model as a function of temperature with  $\alpha = 0.56$ . Figure 9 shows the specific volume for a TGDDM-DDS epoxy as a function of temperature with  $\alpha = 0.875$ . The lower  $\alpha$  value in Figure 8 clearly shows greater expansion of the specific volume with increasing temperature. This aspect is especially noticeable at higher temperatures while at lower temperatures, the specific volumes converge to similar levels.

## B. Thermal conductivity

Since we are interested in multifunctional aspects of materials, another property of interest is thermal conductivity. The dependence of thermal conductivity on nanometer scaled structural details was investigated by a multiscale modeling approach. MD simulation was used to calculate the interfacial thermal resistance between a CNT and the surrounding epoxy matrix as a function of the grafting density of covalently bonded amide functional groups. These amide functional groups participate in the crosslinking chemical reactions shown in Figure 3 such that the CNT becomes part of the crosslinked structure. Figure 10 shows the interfacial thermal resistance as a function of grafting density for the CNT-epoxy composite. Results are similar to those attained previously for an alkane chain group functionalized to a CNT embedded in a linear polymer matrix.<sup>5</sup> The interfacial thermal resistance declines noticeably for a certain range of grafting density ( $\sim 0.008 \text{ \AA}^{-2}$ ) and then appears to decline very little with further increase in the grafting density. This result has some importance, as current synthetic technology may be limited in the amount of grafting density which can be achieved. Furthermore, a high value of the grafting density may result in degradation of various properties of the CNT. Using Equations 10-13, values are predicted for thermal conductivity as a function of grafting density for the CNT for several volumes of CNT loading in the nanocomposite. These calculated thermal conductivity values are plotted in Figure 11. Fairly large increases in the thermal conductivity are predicted for the nanocomposite with moderate loads (5 volume %) of CNT. The strong effect of the functionalization of the CNT surface is seen as the grafting density of this functionalization is increased.

## IV. Conclusions

Structural details at the nanometer length scale can influence macroscopic properties. The results here indicate how atomistic simulation can yield insight into these structure-property relationships. The elastic modulus was calculated for several epoxy systems. The results indicate a dependence of Young's modulus on epoxy matrix molecular structure (difunctional versus tetrafunctional epoxy monomers, degree of crosslinking), on temperature and on the amount of moisture present. The dependence on moisture content remains somewhat elusive due to the complex issues involved. Speculation on these issues in the past has included free volume, moisture-matrix interactions, and statistical issues associated with the MD simulation.<sup>22</sup> Atomistic simulation, combined with a multi-scale modeling approach makes strong predictions for the effect of functionalization on the thermal conductivity of CNT based nanocomposites.

## References

<sup>1</sup>Gates, T. S., Odegard, G. M., Frankland, S. J. V., and Clancy, T. C. "Computational Materials: Multi-scale modeling and simulation of nanostructured materials." *Composites Science and Technology*, Vol. 65, No. 15-16, 2005, pp. 2416-2434.

<sup>2</sup>Theodorou, D. N., and Suter, U. W., "Atomistic Modeling of Mechanical-Properties of Polymeric Glasses" *Macromolecules*, Vol. 19, No. 1, 1986, pp. 139-154.

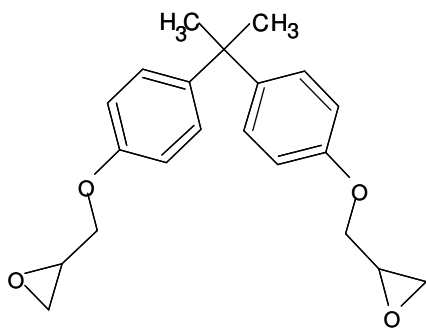
<sup>3</sup>Suter, U. W., and Eichinger, B. E., "Estimating elastic constants by averaging over simulated structures." *Polymer*, Vol. 43, No. 2, 2002, pp. 575-582.

<sup>4</sup>Yarovsky, I., and Evans, E., "Computer simulation of structure and properties of crosslinked polymers: application to epoxy resins." *Polymer*, Vol. 43, No. 3, 2002, pp. 963-969.

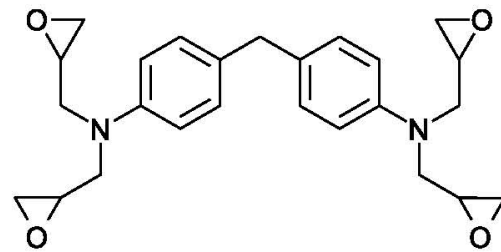
<sup>5</sup>Clancy, T. C., and Gates, T. S., "Modeling of interfacial modification effects on thermal conductivity of carbon nanotube composites." *Polymer* Vol. 47, No. 16, 2006, pp. 5990-5996.

<sup>6</sup>Shenogin, S., Bodapati, A., Xue, L., Ozisik, R., and Keblinski, P., "Effect of chemical functionalization on thermal transport of carbon nanotube composites." *Applied Physics Letters*, Vol. 85, No. 12, 2004, pp. 2229-2231.

- <sup>7</sup>Shenogin, S., Xue, L. P., Ozisik, R., Koblinski, P., and Cahill, D. G., "Role of thermal boundary resistance on the heat flow in carbon-nanotube composites." *Journal of Applied Physics*, Vol. 95, No. 12, 2004, pp. 8136-8144.
- <sup>8</sup>Clancy, T. C., and Gates, T. S., "Mechanical properties of nanostructured materials determined through molecular modeling techniques." *46th AIAA/ASME/ASCE/AHS/ASC Structures, Structural Dynamics and Materials Conference*, Austin, TX, 2005.
- <sup>9</sup>Plimpton, S., "Fast Parallel Algorithms For Short-Range Molecular-Dynamics" *Journal of Computational Physics*, Vol. 117, No. 1, 1995, pp. 1-19.
- <sup>10</sup>Wang, J. M., Cieplak, P., and Kollman, P. A., "How well does a restrained electrostatic potential (RESP) model perform in calculating conformational energies of organic and biological molecules?" *Journal of Computational Chemistry*, Vol. 21, No. 12, 2000, pp. 1049-1074.
- <sup>11</sup>Weiner, P. K., and Kollman, P. A., "AMBER: Assisted Model Building with Energy Refinement. A General Program for Modeling Molecules and Their Interactions" *Journal of Computational Chemistry*, Vol. 2, 1981 pp. 287-303.
- <sup>12</sup>Jorgensen, W. L., Chandrasekhar, J., Madura, J. D., Impey, R. W., and Klein, M. L., "Comparison of Simple Potential Functions for Simulating Liquid Water" *Journal of Chemical Physics*, Vol. 79, No. 2., 1983, pp. 926-935.
- <sup>13</sup>Materials Studio, Software Package, Ver. 2.2, Accelrys Inc., San Diego, CA, 2002
- <sup>14</sup>Wu, C. F., and Xu, W. J., "Atomistic molecular modelling of crosslinked epoxy resin." *Polymer*, Vol. 47, No. 16, 2006, pp. 6004-6009.
- <sup>15</sup>Capaldi, F. M., Boyce, M. C., and Rutledge, G. C., "Molecular response of a glassy polymer to active deformation." *Polymer*, Vol. 45, No. 4, 2004, pp. 1391-1399.
- <sup>16</sup>Lyulin, A. V., Balabaev, N. K., Mazo, M. A., and Michels, M. A. J., "Molecular dynamics simulation of uniaxial deformation of glassy amorphous atactic polystyrene." *Macromolecules*, Vol. 37, No. 23, 2004, pp. 8785-8793.
- <sup>17</sup>Huxtable, S. T., Cahill, D. G., Shenogin, S., Xue, L. P., Ozisik, R., Barone, P., Usrey, M., Strano, M. S., Siddons, G., Shim, M., and Koblinski, P., "Interfacial heat flow in carbon nanotube suspensions." *Nature Materials*, Vol. 2, No. 11, 2003, pp. 731-734.
- <sup>18</sup>Pierson, H. O., *Handbook of Carbon, Graphite, Diamond and Fullerenes: Properties, Processing and Applications*, Noyes Publications, 1994.
- <sup>19</sup>Nan, C. W., Liu, G., Lin, Y. H., and Li, M., "Interface effect on thermal conductivity of carbon nanotube composites." *Applied Physics Letters*, Vol. 85, No. 16, 2004, pp. 3549-3551.
- <sup>20</sup>Berber, S., Kwon, Y. K., and Tomanek, D., "Unusually high thermal conductivity of carbon nanotubes." *Physical Review Letters*, Vol. 84, No. 20, 2000, pp. 4613-4616.
- <sup>21</sup>Berry, N. G., d'Almeida, J. R. M., Barcia, F. L., and Soares, B. G., "Effect of water absorption on the thermal-mechanical properties of HTPB modified DGEBA-based epoxy systems." *Polymer Testing*, Vol. 26, No. 2, 2007, pp. 262-267.
- <sup>22</sup>Goudeau, S., Charlot, M., and Muller-Plathe, F., "Mobility enhancement in amorphous polyamide 6,6 induced by water sorption: A molecular dynamics simulation study." *Journal of Physical Chemistry B*, Vol. 108, No. 48, 2004, pp. 18779-18788.

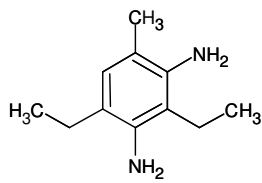


a

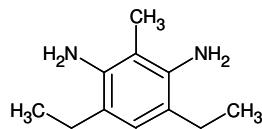


b

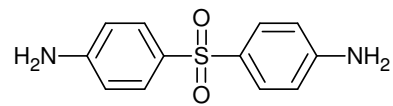
Figure 1. The two epoxy molecules used in the simulation. a) the diglycidyl ether of bisphenol A (DGEBA) b) tetraglycidyl diamino diphenyl methane (TGDDM) .



a



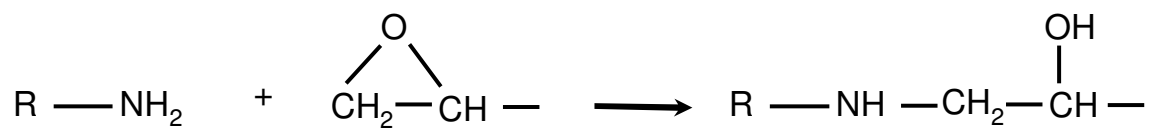
b



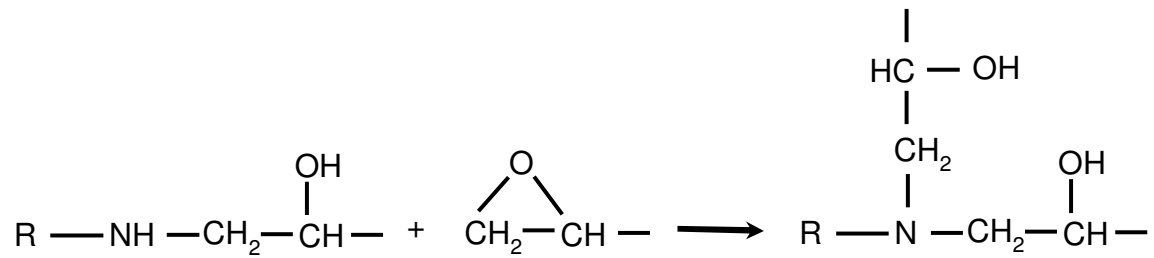
c

Figure 2. The crosslinker molecules used in the simulation. a)-b) the two isomers of diethylene toluene diame (DETDA). c) diamino diphenyl sulfone (DDS).





**a**



**b**

Figure 3. The chemical reactions of an epoxy and an amine. The upper chemical reaction (a) shows the reaction of an amine in a crosslinker molecule reacting with an epoxide group. The lower reaction (b) shows the amine in the product of the upper reaction undergoing a second reaction with another epoxide group resulting in a crosslink.

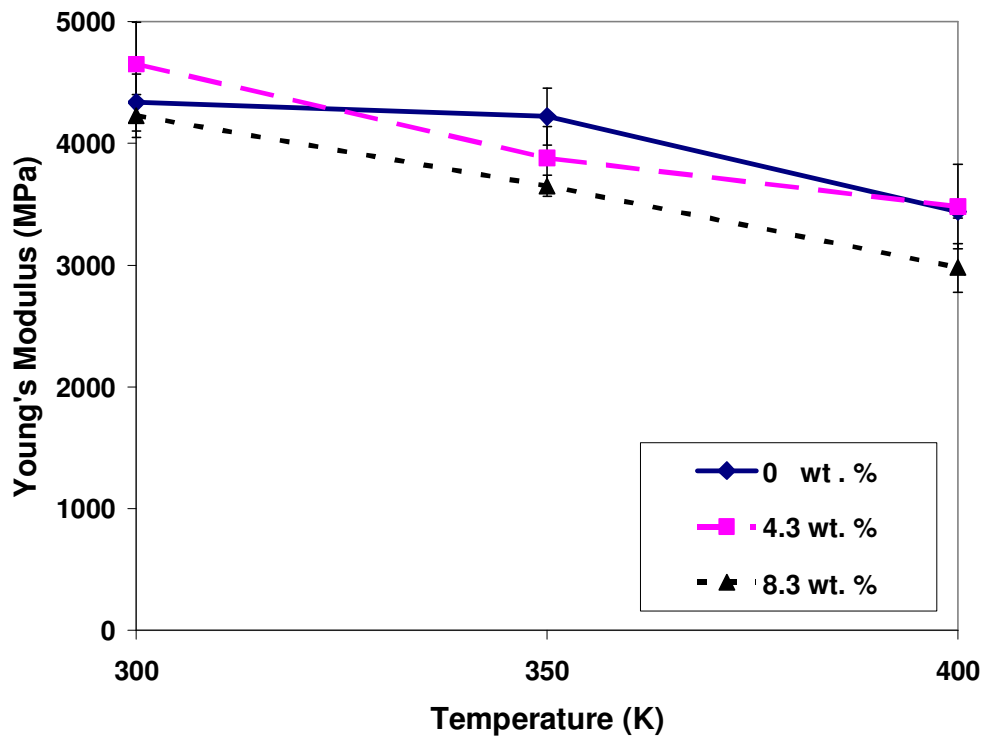


Figure 4. The Young's modulus as a function of temperature for the TGDDM-DDS epoxy with degree of crosslink,  $\alpha = 0.875$ , with varying water content.

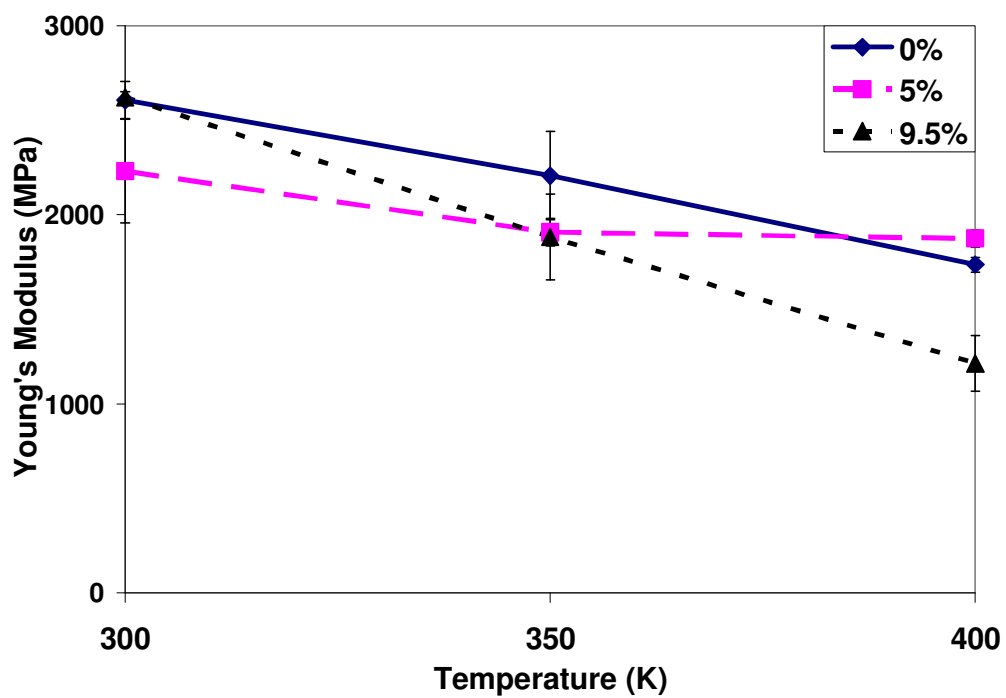


Figure 5. The Young's modulus as a function of temperature for the DGEBA-DETDA epoxy with degree of crosslink,  $\alpha=0.86$ , with varying water content.

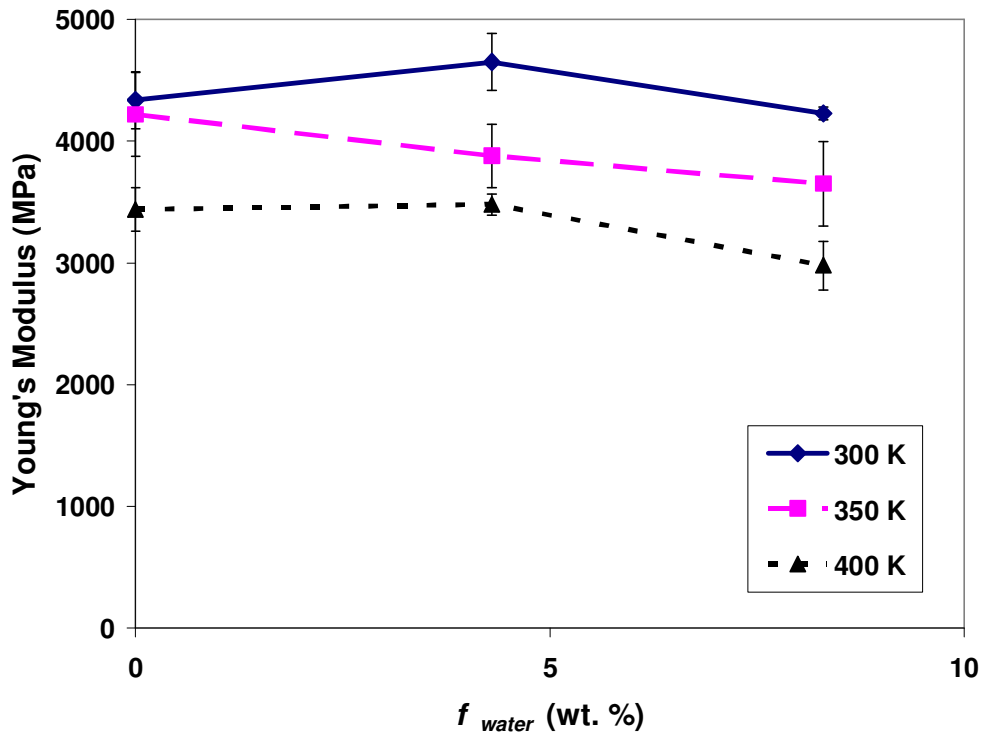


Figure 6. The Young's modulus as a function of water fraction,  $f_{water}$ , for the TGDDM-DDS epoxy with degree of crosslink,  $\alpha = 0.875$ . The curves shown are for 3 different temperatures,  $T = 300$  K, 350 K and 400 K.

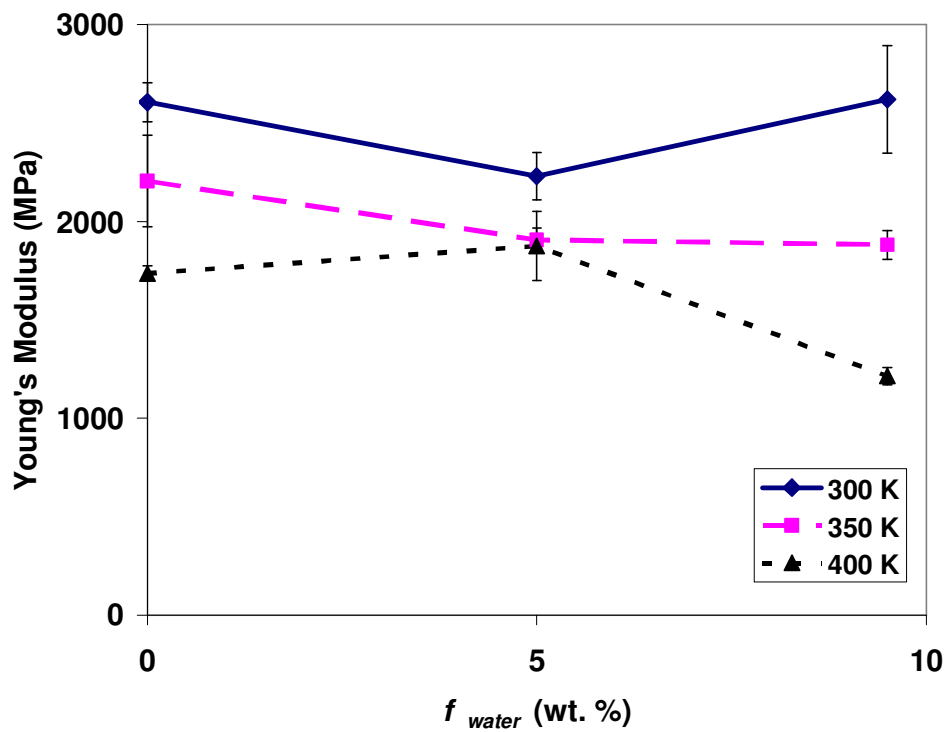


Figure 7. The Young's modulus as a function of water fraction,  $f_{water}$ , for the DGEBA-DETDA epoxy with degree of crosslink,  $\alpha = 0.86$ . The curves shown are for 3 different temperatures,  $T = 300$  K, 350 K and 400 K.

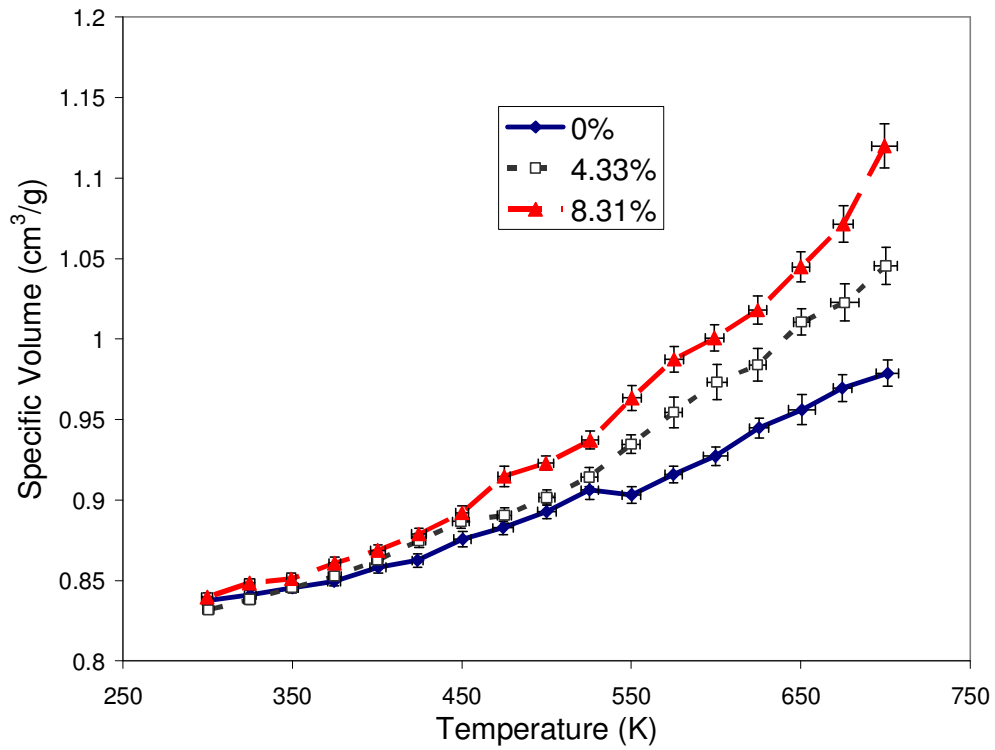


Figure 8. The specific volume as a function of temperature for the TGDDM-DDS epoxy with degree of crosslink,  $\alpha = 0.56$ . The three curves are for models with varying water content,  $f_{water} = 0, 4.33$  and  $8.31$  wt. %.

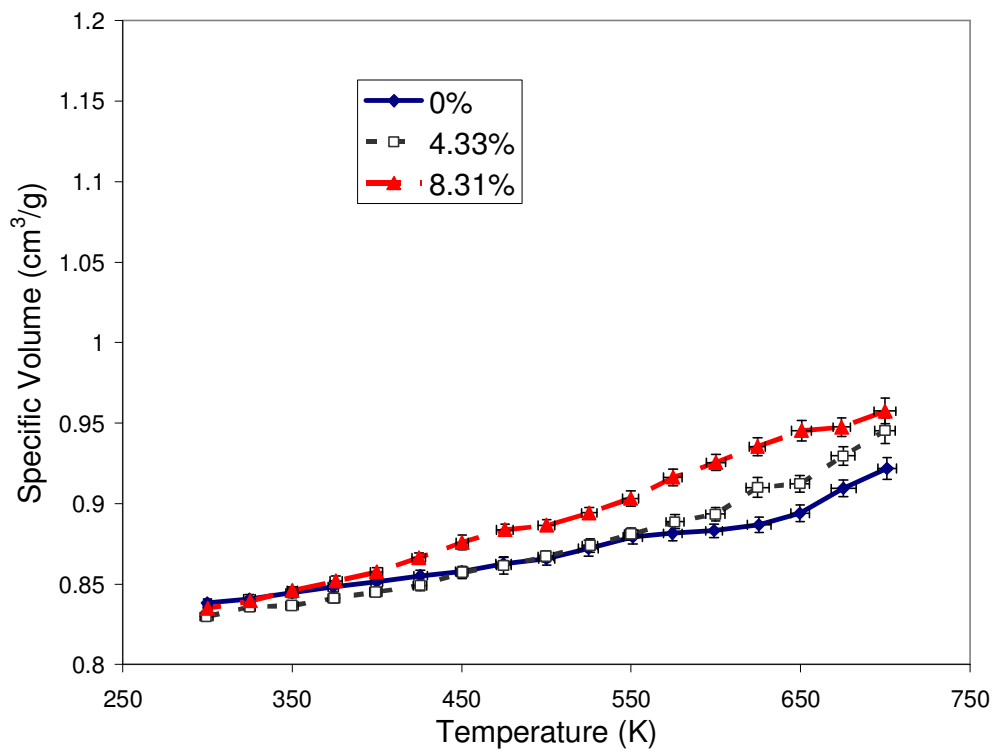


Figure 9. The specific volume as a function of temperature for the TGDDM-DDS epoxy with degree of crosslink,  $\alpha = 0.875$ . The three curves are for models with varying water content,  $f_{water} = 0, 4.33$  and  $8.31$  wt. %.

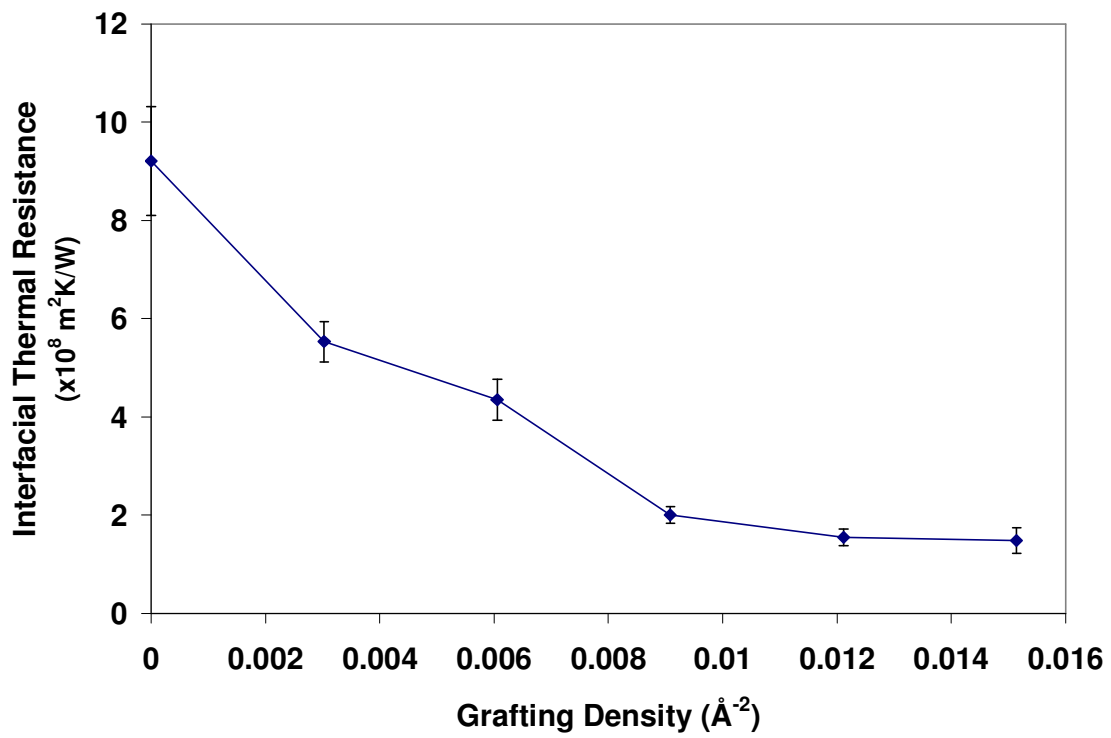


Figure 10. The interfacial thermal resistance,  $R_K$ , between a carbon nanotube and the surrounding matrix as a function of the grafting density of functional groups on the surface of the nanotube.



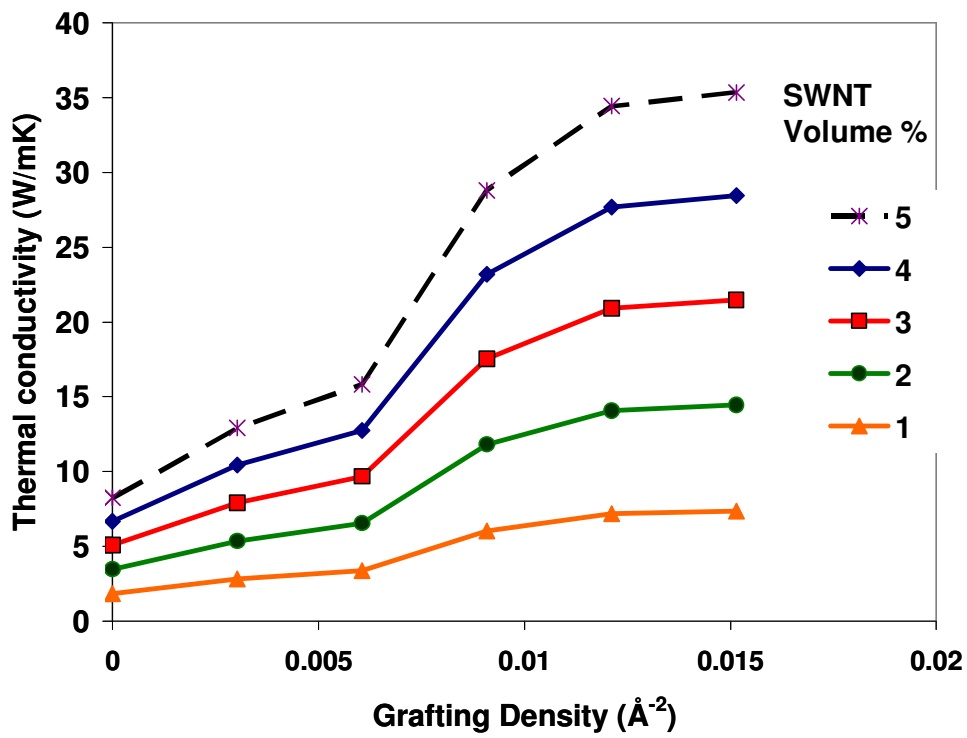


Figure 11. The thermal conductivity of a carbon nanotube-epoxy nanocomposite as a function of the grafting density of functional groups on the surface of the nanotube. The 5 different curves correspond to different values of the nanotube volume fraction assumed.